REPORT DOCUMENTATION PAGE

Form Approved
OMB NO. 0704-0188

1. AGENCY USE ONLY (Leave Blank)	2. REPORT DATE	3. REPORT TYPE AND DATES COVERED
	October 03, 2003	Final Report June 01, 2001 – June 30, 2003

4. TITLE AND SUBTITLE
Synthesis of Bulk Nanostructured Al Alloys with Ultra-high Strength and Wear Resistance for Army Applications

5. FUNDING NUMBERS
DAAD19-01-1-0627

6. AUTHOR(S)
E.J. Lavernia and F.A. Mohamed

7. PERFORMING ORGANIZATION NAME(S) AND ADDRESS(ES)
University of California, Irvine

8. PERFORMING ORGANIZATION REPORT NUMBER

9. SPONSORING / MONITORING AGENCY NAME(S) AND ADDRESS(ES)
U. S. Army Research Office
P.O. Box 12211
4300 S. Miami Blvd.
Research Triangle Park, NC 27709-2211

41912.4-MS

11. SUPPLEMENTARY NOTES
The views, opinions and/or findings contained in this report are those of the author(s) and should not be construed as an official Department of the Army position, policy or decision, unless so designated by other documentation.

12 a. DISTRIBUTION / AVAILABILITY STATEMENT	12 b. DISTRIBUTION CODE
Approved for public release; distribution unlimited.	

13. ABSTRACT (Maximum 200 words)

An Al alloy with a chemical composition of $Al_{85}Ni_{10}La_5$ (at.%) has been selected for exploratory development of new bulk nanostructured Al alloys aiming at ultra-high strength as well as good wear performance for future Army systems. The selected alloy has a high potential to be a candidate due to its inherent good glass forming ability, thermal stability and mechanical properties. Amorphous powders of the $Al_{85}Ni_{10}La_5$ alloy were produced using a gas atomization technique. These powders can be used for synthesizing ultra-high strength bulk nanostructured Al alloy via crystallization from the amorphous phase. In addition, $Al_{85}Ni_{10}La_5$ ribbon was also fabricated using a melt spinning technique. The amorphous alloy of $Al_{85}Ni_{10}La_5$ (at.%) was successfully fabricated in terms of melt-spun ribbons and, particularly, gas-atomized powders (<25μm). The devitrification behavior and kinetics were investigated using SEM, XRD, DSC and TEM etc. Useful information has been obtained for the following consolidation procedure to produce bulk nanostructured Al alloy. It was shown that the $Al_{85}Ni_{10}La_5$ amorphous powders have high thermal stability and a processing at 250°C could result in a grain size of 20~30 nm. Efforts on the investigation of the stabilization mechanisms in bulk nanostructured Al materials were also carried out.

14. SUBJECT TERMS	15. NUMBER OF PAGES
Nanostructured Al alloy, Amorphous Al alloy, Consolidation, Thermal stability, Crystallization, Gas atomization, Melt spinning	
	16. PRICE CODE

17. SECURITY CLASSIFICATION OR REPORT	18. SECURITY CLASSIFICATION ON THIS PAGE	19. SECURITY CLASSIFICATION OF ABSTRACT	20. LIMITATION OF ABSTRACT
UNCLASSIFIED	UNCLASSIFIED	UNCLASSIFIED	UL

REPORT DOCUMENTATION PAGE (SF298)
(Continuation Sheet)

1. List of Publications

(1) Q. Xu and E.J. Lavernia, "Influence of Nucleation and Growth Phenomena on Microstructural Evolution during Droplet-based Deposition" *Acta Materialia,* Vol. 49, pp. 3849-3861, 2001.
(2) S.Q. Armster, J.-P. Delplanque, M. Rein, E.J. Lavernia, "Thermo-fluid mechanisms controlling droplet-based materials processes, " *International Materials Reviews,* Vol. 47, No. 6 pp. 265-301. 2002
(3) A. E. Berkowitz, M. F. Hansen, F. T. Parker, K. S. Veccchio, F. E. Spada, E. J. Lavernia, R. Rodriguez, J. *Magnetism and Magnetic Materials*, Vol. 254-255, pp. 1-6, 2003.
(4) Bing Q. Han, E. J. Lavernia and Farghali A. Mohamed, *Metall. Mater. Trans. A,* Vol. 34, pp. 71-83, 2003.
(5) Z. Zhang, F. Zhou, E. J. Lavernia, "On the analysis of grain size in bulk nanocrystalline materials via X-ray *Metall. Mater. Trans. A*, Vol. 34A, pp. 1349-1355, 2003.

2. Scientific Personnel

Mr. Zhihui Zhang, PhD student
Mr. David Witkin, PhD student
Mr. Kit Foo, PhD Student
Mr. Akshay Verma, MS, 2002
Mr. Darryl Mack, Laboratory Technician (no cost)

3. Scientific Progress and Accomplishments

The objectives of this research program are twofold: first, to establish an in-depth understanding of the factors that govern the synthesis and mechanical behavior of bulk nanostructured materials; second, to utilize this fundamental information to develop new bulk nanostructured Al alloys with ultra-high strength and bulk nanostructured Al alloys with good wear performance for future Army systems. The former is intended for lightweight structural applications and the latter is for high-speed reciprocating and rotating machinery in advanced Army systems, for example, special-purpose Army vehicles for rapid deployment of military contingencies. This report covers the progress made at the University of California, Irvine (UCI), during from July 1, 2001 to June 30, 2003. Please note that this program is being continued at the University of California, Davis (UCD).

3.1 Materials Selection

$Al_{85}Ni_{10}La_5$ in the atomic percent has been selected for the preliminary research activities. The Al-TM(Fe, Co, Ni)-R(rare earth elements) alloys are attractive due to their inherent good glass forming ability, thermal stability as well as mechanical properties. Al-Ni system has a wider chemical composition range of glass forming and thus a better ability to adjust the phase constitution. Lanthanum has good glass forming ability in combination with cost-effectiveness compared to other rare earth metals. Besides high glass forming ability and high mechanical properties for this alloy system, key advantages should also include its characteristic of distinct glass transition, or multistage crystallization, which means that nanocrystallization of the amorphous phase can take place and be controlled under appropriate conditions, thus providing an opportunity for synthesizing bulk nanostructured aluminum alloys using conventional and available P/M techniques, for example, cryomilling, HIP'ing and extrusion.

3.2 Fabrication of Amorphous $Al_{85}Ni_{10}La_5$ Alloy

Besides the alloy design, judicious choice of processing method is necessary to produce an alloy with an amorphous feature. Therefore, selection of synthesis routines here also takes into account the viability for producing alloys for larger scale military and industrial applications rather than just on a laboratory scale. Gas atomization and melt spinning techniques were utilized to produce amorphous Al-Ni-La alloy.

(1) Melt spinning: According to the equilibrium diagram, the melting point of the $Al_{85}Ni_{10}La_5$ alloy is approximately 850°C. However, the melting point of Ni and La is 1455°C and 920°C, respectively. To achieve a uniform composition, a master alloy was first produced. A mixture of pure Al (99.999%), Ni (99.9%) and La (99.8%) with a target composition of $Al_{85}Ni_{10}La_5$ (at.%) was melted using an induction heating unit under a high purity argon atmosphere, and the melt was then poured into a mold at a superheat of 250°C. SEM observation (with XDS analysis) indicated that Al, Ni and La were fully mixed, and the master alloy consists of three phases: Al, Al_3Ni, $Al_{11}La_3$. The master alloy was then used to manufacture melt-spun ribbons.

(2) Gas atomization: Amorphous powders were produced by gas atomization technique available at UCI. Similarly, a mixture of pure Al (99.999%), Ni (99.99%) and La (99.99%) with a target composition of $Al_{85}Ni_{10}La_5$ (at.%) was melted using an induction heating unit under a high purity argon atmosphere, but followed by gas atomization using a high purity helium gas at a pressure of 900 ksi. The melt superheat used for gas atomization is 250°C.

Mean size of the gas atomized powder was less than 30 μm in diameter. Vitrification of the gas atomized powders was characterized using XRD and SEM. Figure 1 shows that XRD line profile of the particles (<25 μm) diffuses and no apparent sharp peaks occur. Morphology of the gas atomized powders is shown in Figure 2(a). We can see that particle surface becomes smoother with decreasing the particle size. The cross-section of the particle is also examined in the BSE mode (see Figure 2b), showing precipitates in larger particles, which were determined as Al_3Ni and $Al_{11}La_3$ by EDS.

Compared to the powders produced by gas atomization, similar results were observed in $Al_{85}Ni_{10}La_5$ ribbons produced by melt spinning.

3.3 Materials Characterization

Size distribution of the $Al_{85}Ni_{10}La_5$ powder was analyzed using a COULTER LS100Q analyzer. The results show that the weight percent of the powders less than 25 μm in diameter is approximately 50%. Inspection of the literature indicates that a powder below 25 μm is likely to be in amorphous state. This is supported by our X-ray diffraction (XRD) analyses, showing no crystalline sharp peak in the XRD patterns. However, an analysis of the overall gas atomized powder shows that crystalline phases form in the coarse powders (>25 μm), and the phases consist of Al, Al_3Ni, $Al_{11}La_3$, consistent with the phase formation in the master alloy. Nevertheless, comparison of the XRD pattern with those reported in the literatures demonstrates that the overall $Al_{85}Ni_{10}La_5$ powder has a significant proportion of amorphous phase.

A study of grain growth of nanostructured pure Al compact was also conducted. Previous studies of the cryomilled pure Al powder (mechanical milling under an atmosphere of liquid nitrogen) had revealed a significant stabilization against thermal annealing of grain growth, i.e., the grain size can be maintained at a stable value around 50 nm at temperatures up to as high as 0.78 T/T_M. This provides an opportunity that these powders can be compacted into bulk form with the grain size remaining at the regime of nanoscale without significant coarsening. Furthermore, understanding of the grain growth of pure Al compact can provide valuable insight for the structure evolution in Al-Ni-La alloy. The as-HIP'ed and as-extruded Al bulk samples were isothermally annealed at temperatures of 300°C, 400°C and 500°C, respectively. The integral breadth method was utilized to analyze the grain size of HIP'ed samples from the XRD line profile and Sherrer equation to the extruded sample. XRD results show that both the HIP'ed samples and extruded samples are stable and no significant grain growth has been observed below 0.61 T/T_M, or the temperature of 300°C. These results suggest that the tendency for grain growth in the HIP'ed samples is smaller than that of the extruded ones at temperatures above 300°C.

3.4 Crystallization Behavior and Kinetics of $Al_{85}Ni_{10}La_5$ Alloy

3.4.1 Temperature scan

Findings by DSC analysis are summarized (Figure 3):

(a) A similar crystallization behavior was found for both powders and ribbons.

(b) Clearly divided multi-stages of crystallization were identified, providing a potential to control the crystallization progress, and in turn, may facilitate the subsequent consolidation process.

(c) Intensive primary crystallization behavior, suggesting that a homogeneous dispersion of nanocrystalline particles may be obtained in the amorphous matrix. Nanocrystalline precipitates with a grain size of about 20~30 nm can be exploited as the primary strengthening phase in the ultrahigh strength bulk nanostructured/amorphous Al alloy.

(d) Distinct glass transition features, $T_g \approx 259°C$.

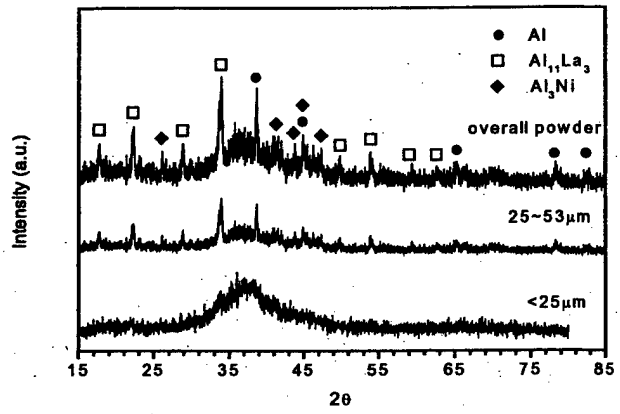

Figure 1 XRD profile of gas atomized $Al_{85}Ni_{10}La_5$ powders.

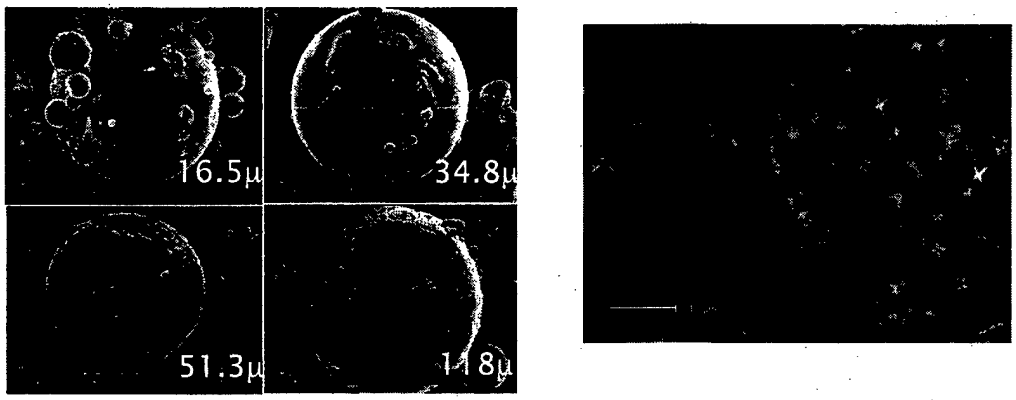

Figure 2 SEM micrographs of the gas atomized $Al_{85}Ni_{10}La_5$ powders: (a) Surface morphology of particles with various sizes (Left); and (b) cross-section image in BSE mode (Right).

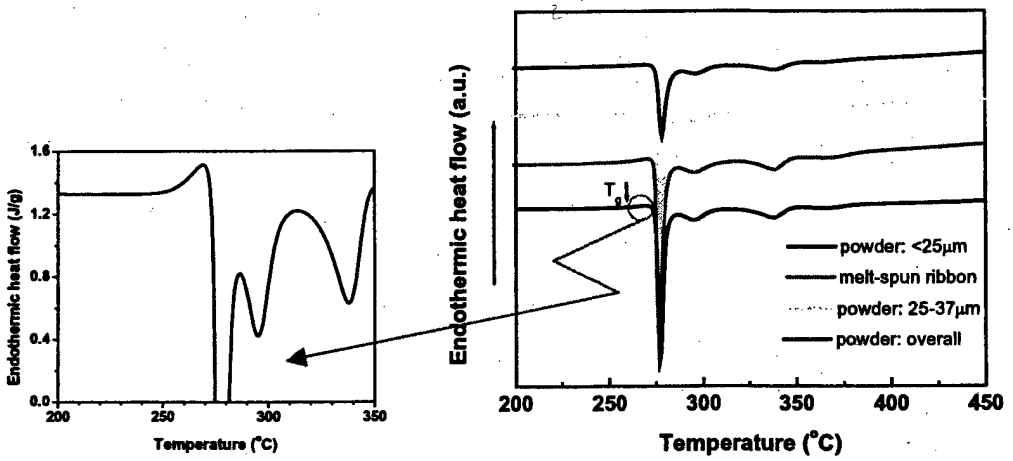

Figure 3 DSC curve of gas atomized $Al_{85}Ni_{10}La_5$ powders.

3.4.2 Kissinger analysis

Results, obtained by fitting the exothermic peak temperature to Kissinger Equation, are shown in Figure 4. Activation energy corresponding the first peak of the $Al_{85}Ni_{10}La_5$ powder (< 25 μm) is approximately E_a=344 KJ/mol. However, the self-diffusion activation energy of Al is Q=144.2 KJ/mol, which is far below the activation energy E_a=344 KJ/mol. It suggests that the presence of the element La and Ni in the amorphous matrix considerably influences precipitating of Al. This may account for the high glass transition point of Tg ≈ 259°C (> $0.55T_M$). The reason why the second peak does not exhibit a good linear relation will be discussed later on.

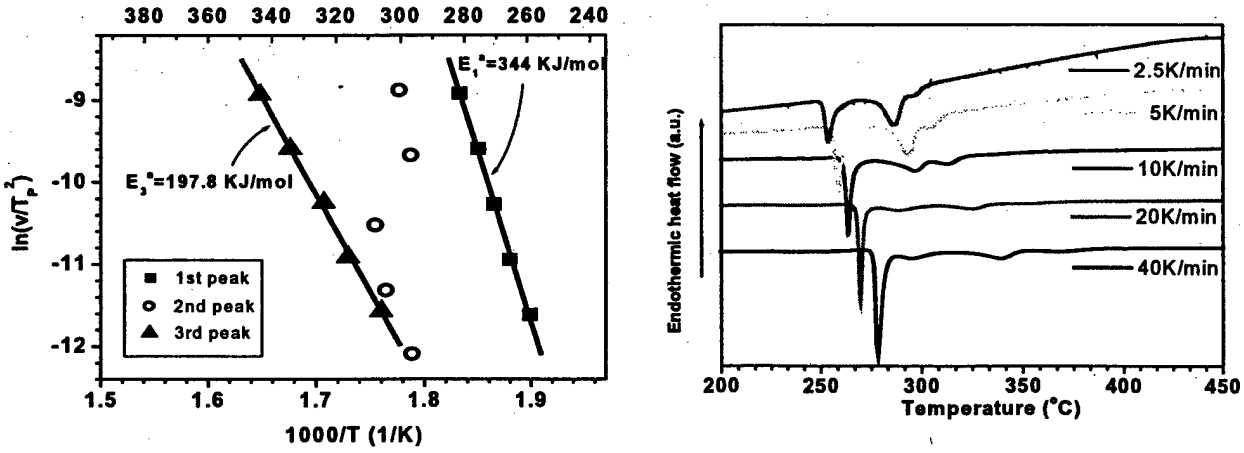

Figure 4 Kissinger plots of gas atomized $Al_{85}Ni_{10}La_5$ powders.

3.4.3 Isothermal scan

Results of isothermal annealing are shown in Figure 5. Please note that sample (a) was annealed for 60 min, sample (b) and (c) for 30 min, and then heated at 40°C /min to 500°C. It can be seen that a primary crystallization peak occurs in sample (a), whereas no apparent primary crystallization peak in (b) and (c). Annealing of the amorphous powders at 235°C, 245°C, 250°C and 283°C, as shown in Fig. 5 may facilitate to investigate their crystallization behavior.

As mentioned above, the size of strengthening phase in the ultrahigh strength bulk nanostructured/amorphous Al alloy is expected to be about 20~30 nm. The inverse Hall-Petch phenomenon may occur when the grain size drops below this range. Thus, processing temperatures must be carefully selected based on the stability of the nanocrystallized phases.

Figure 5 Isothermal annealing of gas atomized $Al_{85}Ni_{10}La_5$ powders.

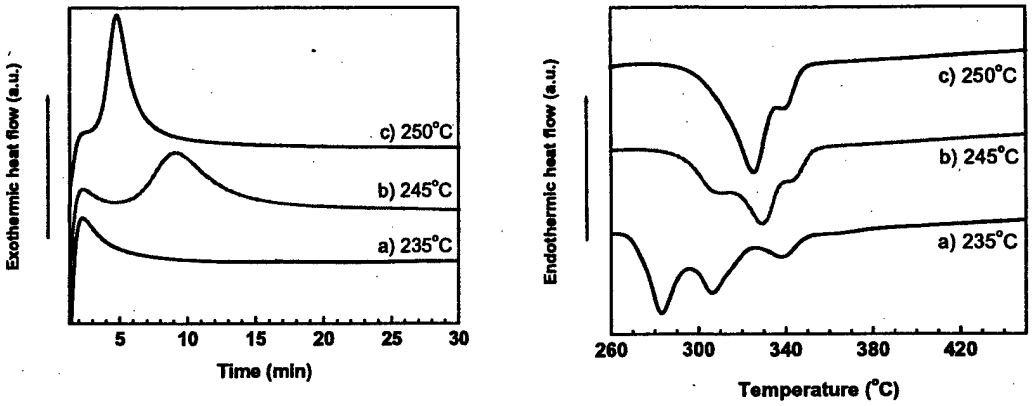

3.4.4 Identification of the Al-La phase during crystallization

Nanoscale-crystallites precipitated during the crystallization process can function as mechanical property strengthening phases. However, it is challenging to identify the crystallized phases in the partially devitrified powders due to presence of the amorphous hump and peak overlapping, for instance, to distinguish the $Al_{11}La_3$ and Al_4La phase. This issue can be overcome by means of analyzing the fully crystallized powder. Results obtained from observation of fully crystallized $Al_{85}Ni_{10}La_5$ powders indicate that:

(a) The Al-La phase is $Al_{11}La_3$;
(b) Fully crystallized $Al_{85}Ni_{10}La_5$ consists of Al , Al_3Ni and $Al_{11}La_3$;
(c) No other intermetallic compounds were found.

3.4.5 Identification of various crystalline phases

XRD analysis of the $Al_{85}Ni_{10}La_5$ powder which was annealed at 235°C, 245°C and 250°C shows that (Figure 6):

(a) Al begins to crystallize at 235°C;
(b) Intermetallic compounds start to precipitate at 245°C. Phases precipitated at this temperature consist of Al, $Al_{11}La_3$, Al_3Ni and Al_3La;
(c) Crystallization behavior at 250°C is similar to that at 245°C;
(d) The Al_3La phase occurs at intermediate temperatures (~250°C) but dissolved at elevated temperatures (283°C);
(e) Phases crystallized at 283°C are the same as those after full crystallization.

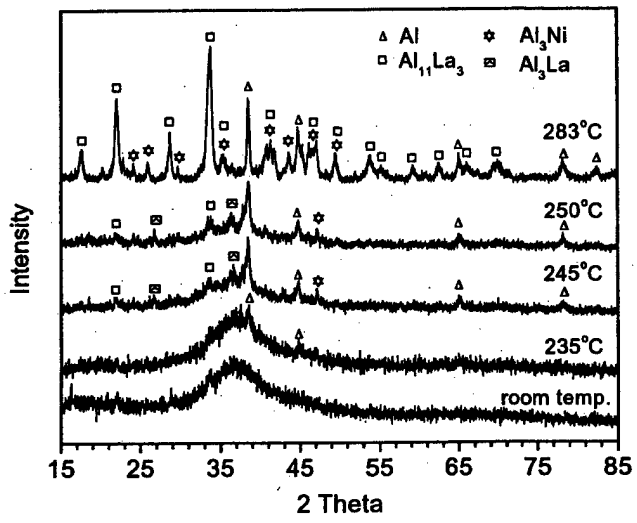

Figure 6 XRD pattern of $Al_{85}Ni_{10}La_5$ powders (<25μm) annealed at various temperatures.

3.5 Thermal Stability Enhancement

3.5.1 Pre-annealing

During the consolidation process, a temperature of approximately 300°C would be optimal to processing of the $Al_{85}Ni_{10}La_5$ powders (degassing, HIP'ing and extrusion etc.). However, a direct processing of the $Al_{85}Ni_{10}La_5$ powder at this temperature may lead to crystallizing and grain coarsening. A TEM observation demonstrated that the grain size could grow to be greater than 300nm. In the present study, it was found that the thermal stability could be improved by pre-annealing. Experimental results suggest that:

(a) An amorphous hump takes place in the XRD profile for pre-annealed $Al_{85}Ni_{10}La_5$ powders (Figure 7);
(b) Presence of Al_3La implies that the microstructure has not been fully evolved, indicating that the stability is enhanced by means of pre-annealing (Figure 7);
(c) Annealing at 250°C without pre-annealing will not cause full crystallization (Figure 5, Figure 6).

3.5.2 Influence of pre-annealing time

The crystallization process is also affected by the pre-annealing time. In Figure 8, the $Al_{85}Ni_{10}La_5$ powder was first pre-annealed at 235°C and then heated to 283°C at a heating rate of 40°C/min. It was found that an increasing of the pre-annealing time from 30 min to 60 min results in a peak shift from 277°C to 283°C. It may be attributed to that pre-annealing helps to improve the thermal stability of the microstructures.

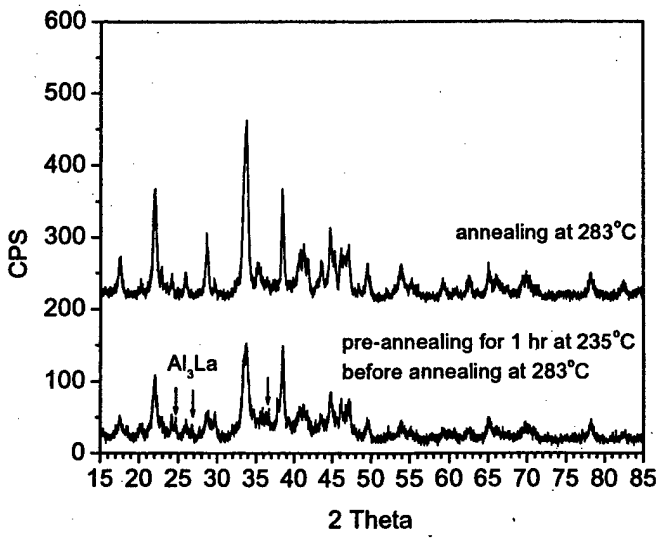

Figure 7 XRD pattern demonstrating the effects of pre-annealing

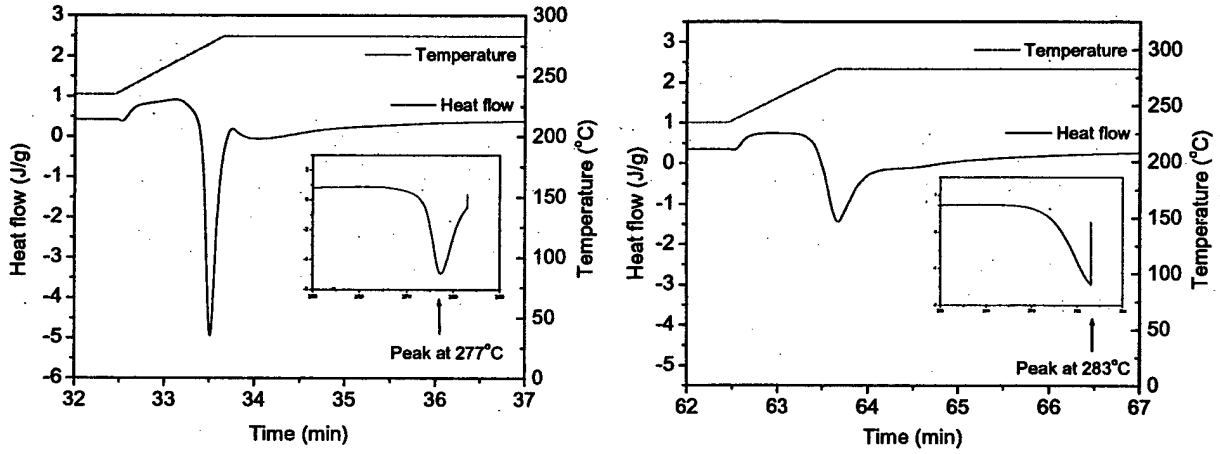

Figure 8 DSC curve demonstrating the effects of pre-annealing time (at a heating rate of 40°C/min).

3.5.3 Primary crystallization peak

It was found that the first crystallization peak does not only correspond to crystallization of the Al phase, but to a combined precipitation process of Al phase and $Al_{11}La_3$ phase. Experimental evidences include:

(a) A Kissinger analysis indicated that the activation energy corresponding to the first peak of the $Al_{85}Ni_{10}La_5$ powder (< 25 μm) is approximately E_a=344 KJ/mol, which is much higher than the Al self-diffusion activation energy of ~144.2 KJ/mol;
(b) At temperatures less than 283°C, XRD peaks for Al_3Ni are not defined as well as those for $Al_{11}La_3$;
(c) Evolution of $A1_{11}La_3$ peaks could be more clearly seen than that of Al_3Ni when the annealing time at 250°C is increased to 3 hr or when the annealing temperature is increased from 250°C to 263°C;
(d) Pre-annealing affects the XRD profile of Al_3Ni phase, whereas the $Al_{11}La_3$ peak is well defined and less affected by pre-annealing;
(e) The first crystallization peak actually consists of two peak overlapping, this could only be revealed at a high heating rate (80°C /min), as seen in Figure 9.

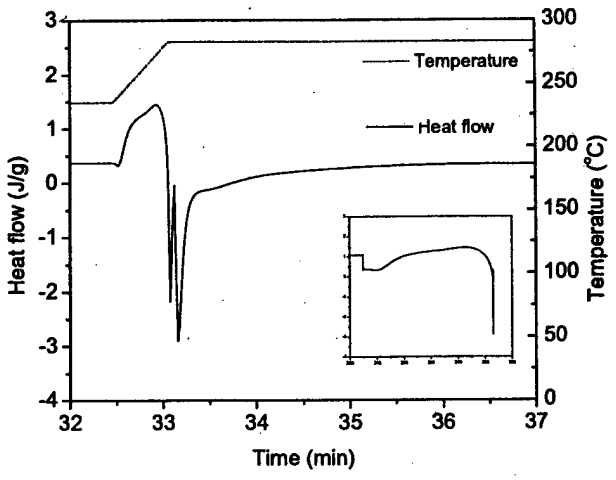

Figure 9 DSC curve showing the first peak reaction at a high heating rate of 80°C /min

3.6 Grain Growth

A study of grain growth was done at selected temperatures of 250°C, 268°C and 280°C. Temperature selections are based on: (1) at the very low heating rate of 2.5°C/min, the onset temperature of the first peak is 250°C and the onset temperature of the second peak is 268°C (Figure 4); (2) intermetallic compound precipitation takes place when annealing at 250°C (Figure 6); (3) full crystallization takes place when annealing at about 280°C (Figure 6). The grain size is determined by TEM observation. Results are shown in Figures 10~13. A further investigation concerning the grain growth is being conducted in combination with the X-ray technique.

(a) When annealing at 250°C for 3 hr, the grain size is about 20~30 nm;
(b) When annealing at 250°C for 6 hr, the grain size is about 40~50 nm;
(c) When annealing at 263°C, a significant grain growth may occur;
(d) When annealing at 280°C for 3 hr, the grain size is about 200-300 nm.

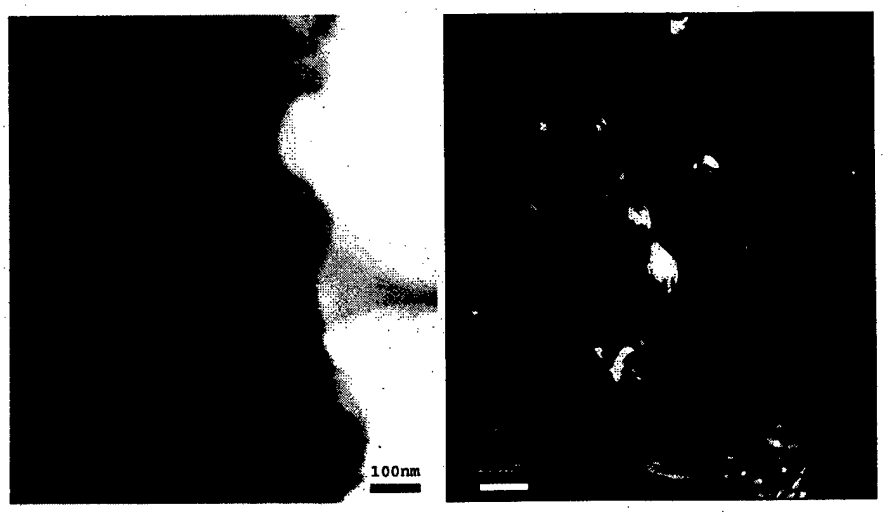

Figures 10 Powder particles (<25 μm) that heat-treated for 250°C for 3 hrs: (a) Bright field (Left); and (b) Dark field (Right).

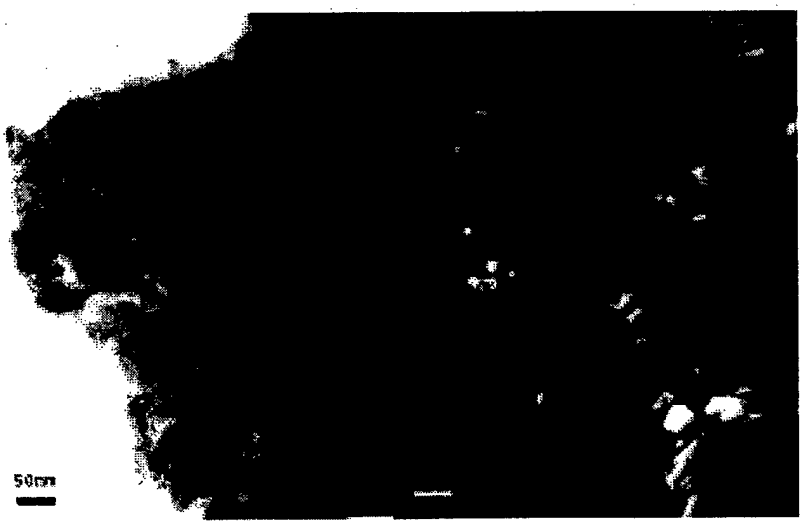

Figures 11 Powder particles (<25 μm) that heat-treated for 250°C for 6 hrs and followed by a holding at 268°C for 3 hrs: (a) Bright field (Left); and (b) Dark field (Right).

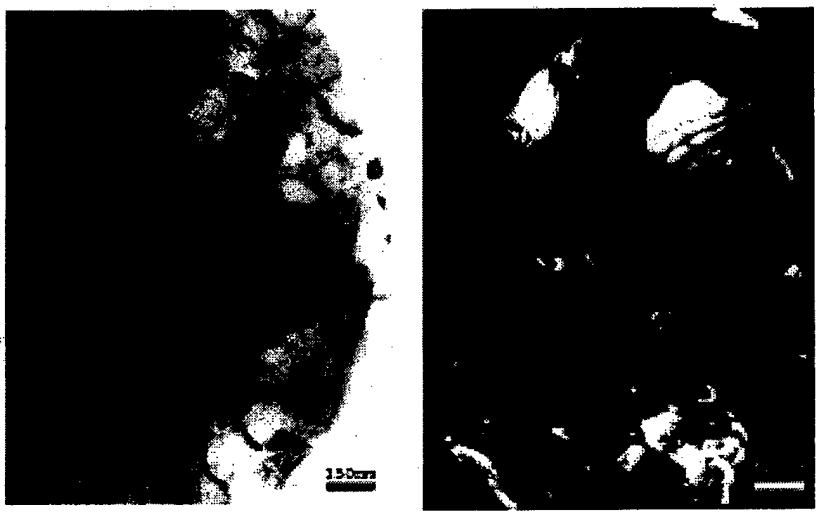

Figure 12 Powder particles (<25 μm) that heat-treated for 250°C for 6 hrs and followed by a holding at 268°C for 6 hrs: (a) Bright field (Left); and (b) Dark field (Right).

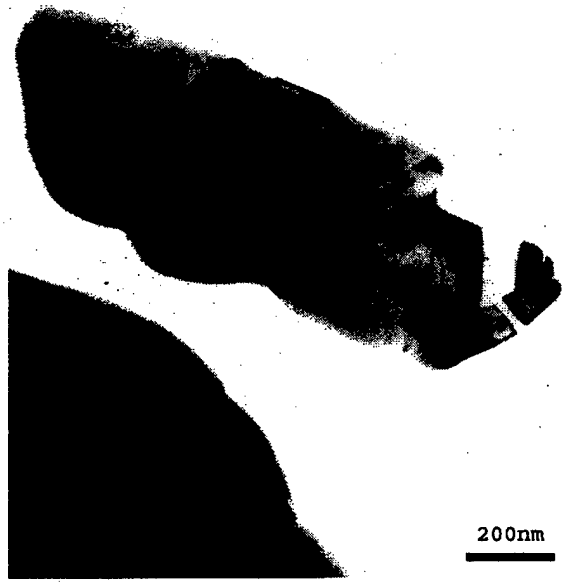

Figure 13 Powder particles (<25 μm) that heat-treated for 280°C for 3 hrs (Bright field).